Journal of Power Sources 240 (2013) 338–343

Contents lists available at SciVerse ScienceDirect

Journal of Power Sources

journal homepage: www.elsevier.com/locate/jpowsour

Preparation and electrochemical performances of nanostructured $Co_xNi_{1-x}(OH)_2$ composites for supercapacitors

Xinwei Liu, Jichun Huang, Xiaopei Wei, Congli Yuan, Tong Liu, Dianxue Cao, Jinling Yin, Guiling Wang*

Key Laboratory of Superlight Material and Surface Technology of Ministry of Education, College of Material Science and Chemical Engineering, Harbin Engineering University, Harbin 150001, PR China

HIGHLIGHTS

- Nanostructured $Co_xNi_{1-x}(OH)_2$ were prepared by a simple hydrothermal process.
- The $Co_xNi_{1-x}(OH)_2$ composites show a greatly improved rate performance.
- $Co_{0.116}Ni_{0.884}(OH)_2$ electrode has a specific capacitance of 1464.7 F g^{-1} at 1 A g^{-1}.

ARTICLE INFO

Article history:
Received 20 January 2013
Received in revised form
27 February 2013
Accepted 7 April 2013
Available online 18 April 2013

Keywords:
Nickel hydroxide
Cobalt
Composites
Nickel foam
Supercapacitors

ABSTRACT

Nanostructured $Co_xNi_{1-x}(OH)_2$ ($x = 0$, 0.053, 0.068, 0.116, 0.192) composites are synthesized via a simple template-free growth process onto nickel foam by using a mixed aqueous solution of nickel nitrate, cobalt nitrate and ammonia. Their structure and surface morphology are characterized by X-ray diffraction, energy dispersive X-ray spectroscopy and scanning electron microscopy. The SEM images show changes in the microstructure of β-$Ni(OH)_2$ by the doping of cobalt. The effects of cobalt content on the electrochemical behaviors of β-$Ni(OH)_2$ are investigated by cyclic voltammetries, galvanostatic charge/discharge and electrochemical impedance spectroscopy. The results show that the $Co_{0.116}Ni_{0.884}(OH)_2$ composite electrode exhibits a drastic improvement in the capacitive characteristics of β-$Ni(OH)_2$ with a specific capacitance increase from 386.4 to 1082.6 F g^{-1} at a high discharging current density of 6 A g^{-1}. This work suggests that the as-prepared $Co_{0.116}Ni_{0.884}(OH)_2$ composite electrode has a promising future as higher charging/discharging rate materials for pseudo-supercapacitors.

1. Introduction

Supercapacitors, also called electrochemical capacitors (ECs), have been attracted much attention as one of the most promising electrical energy storage systems due to their higher power density and longer cycle life than secondary batteries in addition to their higher energy density compared to conventional electrical double-layer capacitors [1–4]. By now, supercapacitors, have been extensively applied in many fields, ranging from portable consumer electronics and computer memory backup systems, to hybrid electric vehicles (HEVs) and EVs [5,6]. On the basis of energy storage mechanisms, ECs can be classified into two categories: electrochemical double layer capacitors (EDLCs), with carbon-based materials as active materials, and pseudocapacitors, with transition metal oxides (RuO_2, MnO_2, NiO, Co_3O_4, CuO, etc.) and hydroxides ($Ni(OH)_2$, $Co(OH)_2$, etc.), or conducting polymers as active materials [7–18]. Particularly, ECs based on RuO_2 oxides exhibit much better capacitance properties (710–1300 F g^{-1} from a single electrode) than conventional carbon materials (75–175 F g^{-1} for aqueous electrolytes and 40–100 F g^{-1} for organic electrolytes) and electronically conducting polymer materials due to its wide potential window, highly reversible redox reactions, high proton conductivity, remarkably high specific capacitance, good thermal stability and long cycle life [5]. However, the high cost of these precious metal materials limits them from commercialization. Therefore, many efforts have been made to search for alternative inexpensive electrode materials with outstanding capacitive characteristics.

Recently, nanostructured composite materials, such as composites of metal oxides (Co_3O_4@MnO_2 [19], MnO_2–NiO [20], etc.) and binary metal oxides/hydroxides ($Ni(OH)_2$–MnO_2 [21], Co_3O_4–$Ni(OH)_2$ [22], etc.), have attracted much interest for supercapacitors because of their enhanced characteristics over the single material. For example, the

* Corresponding author. Tel./fax: +86 451 82589036.
E-mail address: wangguiling@hrbeu.edu.cn (G. Wang).

0378-7753/$ – see front matter © 2013 Elsevier B.V. All rights reserved.
http://dx.doi.org/10.1016/j.jpowsour.2013.04.029

substitution of cobalt compounds into nickel systems can contribute to the increase of electronic conductivity because the effect of d-electrons of Ni(II) and CoOOH can serve as a good current collector [22]. In addition, some other beneficial effects also have been found, for instance, reducing the mechanical stress during charge/discharge processes, in the result of preventing electrode failure as well as increasing the charge density. $Ni(OH)_2$ is a promising electrode material for applications in supercapacitors due to its well defined electrochemical redox activity, low environmental pollution, low cost and high theoretical specific capacitance. However, its specific performance at higher charging/discharging current density was unsatisfactory. It was observed that the double metal hydroxide $Co(OH)_2/Ni(OH)_2$ can inherit the advantages of both cobalt and nickel hydroxide and has superiority over either of the single hydroxide.

Hence, in this study, nanostructured $Co_xNi_{1-x}(OH)_2$ (x = 0, 0.053, 0.068, 0.116, 0.192) composites attached on nickel foam are synthesized via a simple template-free growth method. The $Co_{0.116}Ni_{0.884}(OH)_2$ composites electrode exhibits highest specific capacitance of 1464.7 F g^{-1} at 1 A g^{-1} and 1082.6 F g^{-1} at 6 A g^{-1}, indicating that $Co_{0.116}Ni_{0.884}(OH)_2$ composites have a promising future as potential electrode material for pseudo-supercapacitors.

2. Experimental

All the chemicals used in our experiments were purchased and used as received without any purification. For the synthesis of $Co_xNi_{1-x}(OH)_2$ composite materials on nickel foam, a method called template-free growth was used. In this typical synthesis process [23–25], $Ni(NO_3)_2\cdot 6H_2O$, $Co(NO_3)_2\cdot 6H_2O$ and 5 mmol NH_4NO_3 were dissolved in 35 cm^{-3} deionized water. The mass ratio of Co^{2+} in solution was set at 0%, 5%, 10%, 15% and 20%. Then 18 cm^{-3} ammonia (25 wt%) was added to that solution under vigorous stirring to obtain the growth solution. Then the solution was transferred into a petri dish and heated at 90 °C for 2 h in an oven. After that, a piece of nickel foam (10 mm × 10 mm × 1.1 mm, 110 PPI, 320 g m^{-2}, Changsha Lyrun Material Co., Ltd. China) was immersed in the growing solution for 12 h at 90 °C to prepare the $Co_xNi_{1-x}(OH)_2$ composite materials. Prior to use, the nickel foam was pretreated by degreasing in acetone for 10 min, etching in 6.0 mol dm^{-3} HCl for 15 min, washing with deionized water, soaking in 0.1 mmol dm^{-3} $NiCl_2$ for 4 h, and washing again thoroughly with deionized water. After growth, the electrodes were washed with deionized water and dried at 60 °C in a vacuum oven for 2 h to get the samples of $Co_xNi_{1-x}(OH)_2$ electrode. The structure of the $Co_xNi_{1-x}(OH)_2$ composite materials was analyzed using X-ray diffractometer (XRD, Rigaku TTR III) Cu K_α radiation (λ = 0.1506 nm). The 2θ ranges from 10° to 90° with a scan rate of 10° min^{-1} and a step width of 0.02°. The surface morphology of $Co_xNi_{1-x}(OH)_2$ composite materials was examined by scanning electron microscope (SEM, JEOL JSM-6480) equipped with an energy-dispersive X-ray (EDX) analyzer.

Electrochemical measurements were performed in a conventional three-electrode electrochemical cell. The prepared electrode (1 cm^2 nominal planar area) acted as the working electrode, a platinum foil (1 cm × 2 cm) served as the counter electrode, and a saturated calomel electrode (SCE) was used as the reference electrode. The cyclic voltammetries (CVs) and electrochemical impedance spectroscopy (EIS) were performed using a computerized VMP3/Z potentiostat (Bio-Logic) controlled by the EC-lab software. The galvanostatic charge/discharge tests were conducted on a LAND battery program-control test system. All electrochemical measurements were performed in 6 mol dm^{-3} KOH electrolyte. All solutions were made with analytical grade chemical reagents and Millipore Milli-Q water (18 MΩ cm). Electrochemical impedance spectroscopy (EIS) measurements were carried out by applying an AC voltage with 5 mV amplitude in a frequency range from 0.01 Hz to 100 kHz at the open circuit potential.

Table 1
EDX analysis of Co content in β-$Ni(OH)_2$ as compared to Co content in the initial solutions of $Ni(NO_3)_2\cdot 6H_2O$ and $Co(NO_3)_3\cdot 6H_2O$.

Co content in solution [Co/Ni + Co] (Wt%)	Co content in solution [Co/Ni + Co] (mol%)	Co content in sample [Co/Ni + Co] (mol%)
5	6.2	5.3
10	7.1	6.8
15	15.8	11.6
20	30.0	19.2

3. Results and discussion

3.1. Characterization of $Co_xNi_{1-x}(OH)_2$ electrode

The mol content of cobalt in the initial solution as well as in the prepared $Co_xNi_{1-x}(OH)_2$ electrode, obtained by means of EDX analysis, is given in Table 1. It can be seen that the content of Co is proportional to that in the initial solution. In the following text, the composite materials are abbreviated as $Co_xNi_{1-x}(OH)_2$, with x = 0.053, 0.068, 0.116 and 0.192. It was found that the mol content of Co increases with the increase in the initial solution, revealing the substitution of Ni of the materials. Fig. 1 shows the XRD patterns of the as-prepared β-$Ni(OH)_2$ and $Co_xNi_{1-x}(OH)_2$ (x = 0.053, 0.068, 0.116 and 0.192) composites powder scratched from nickel foam. Before the doping of Co^{2+}, the XRD pattern matches well with the standard crystallographic spectrum of hexagonal β-$Ni(OH)_2$ (JCPDS card No. 14-0117). The lattice constants were calculated to be $a = b$ = 0.3123 nm and c = 0.4610 nm for the sample; they are consistent with the standard values of β-$Ni(OH)_2$ ($a = b$ = 0.3126 nm, and c = 0.4605 nm). The effect of Co^{2+} can be noticed in the X-ray diffraction patterns. It was found that the diffraction peaks position of $Co_xNi_{1-x}(OH)_2$ did not change obviously with the addition of Co^{2+}. This is due to the similar metal ionic radius between nickel and cobalt. As the mol content of Co^{2+} in β-$Ni(OH)_2$ was increased, the diffraction intensity of diffraction peak (100) decreased slightly, while the diffraction intensity of $Co_{0.192}Ni_{0.808}(OH)_2$ increased slightly. It was noted that no other diffraction peaks from impurities

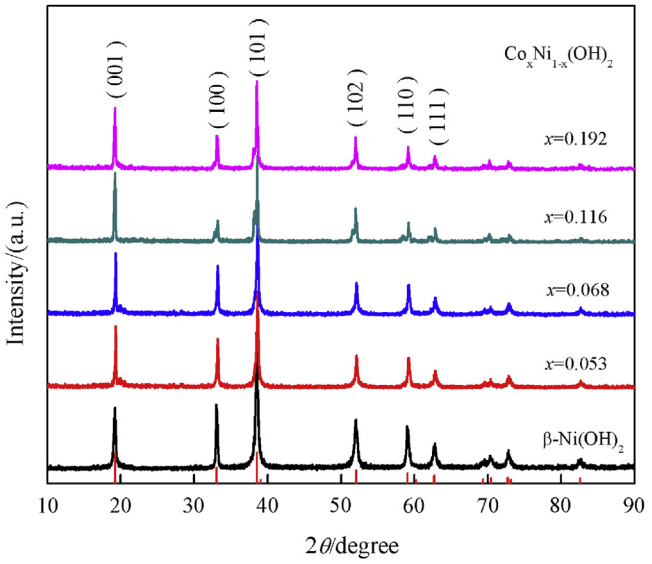

Fig. 1. XRD patterns of β-$Ni(OH)_2$ and $Co_xNi_{1-x}(OH)_2$ composite materials scratched down from the nickel foam.

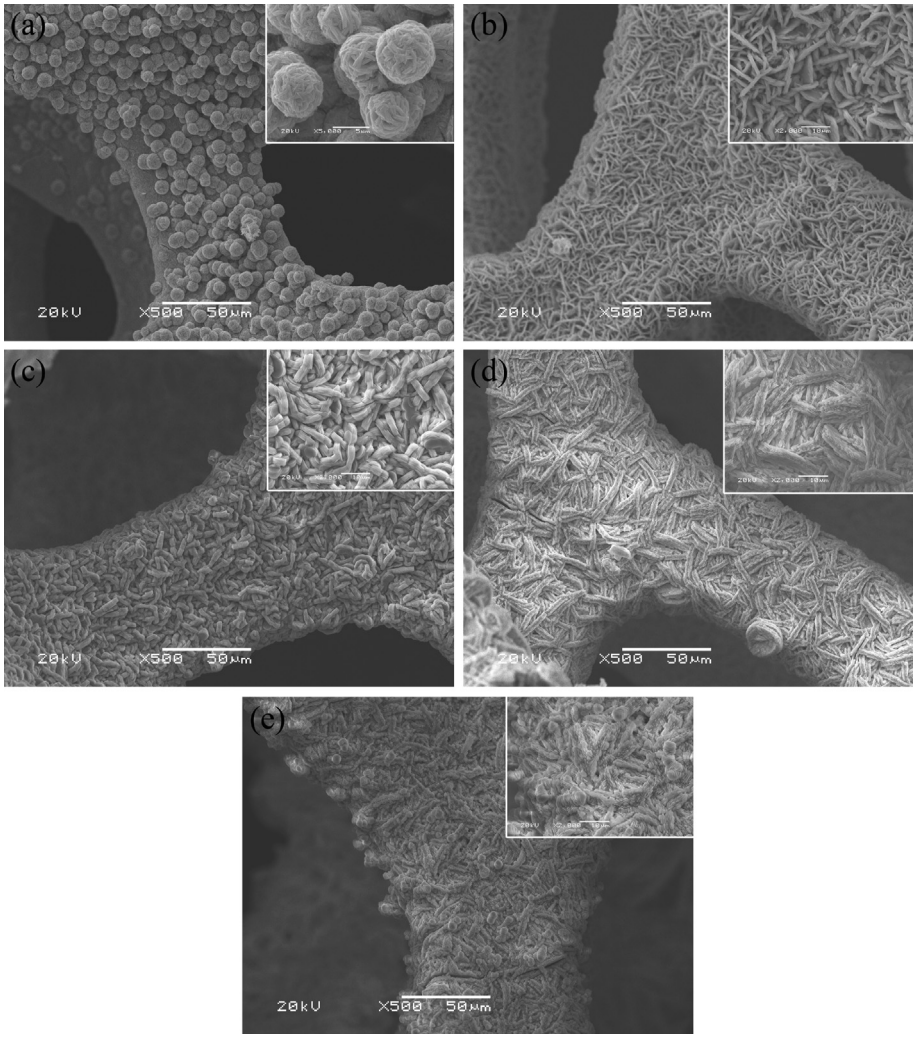

Fig. 2. The SEM images of the $Co_xNi_{1-x}(OH)_2$ with x values of (a) 0, (b) 0.053, (c) 0.068, (d) 0.116 (e) 0.192.

were observed, especially Co_3O_4, indicating the addition of Co^{2+} did not affect the crystal structure of β-phase $Ni(OH)_2$ significantly.

Fig. 2 shows the SEM images of β-$Ni(OH)_2$ and $Co_xNi_{1-x}(OH)_2$ composites attached on nickel foam. Fig. 2a shows that β-$Ni(OH)_2$ presents on the nickel foam skeleton mostly as spherical clusters, which have relatively uniform size with a diameter of ~5 μm. The β-$Ni(OH)_2$ spheres are actually composed of many nanoribbons, which consist of nanosheets. However, the spherical β-$Ni(OH)_2$ disappeared when Co^{2+} was added. The nanoribbons uniformly tiled on nickel foam, respectively, as seen in Fig. 2b–e. When the mol content of Co in β-$Ni(OH)_2$ was 6.8 mol% ($Co_{0.068}Ni_{0.932}(OH)_2$), the active material attached on the nickel foam was converted to uniform film (Fig. 2c). No obvious changes were observed upon increasing the cobalt up to 11.6 mol% ($Co_{0.116}Ni_{0.0.884}(OH)_2$) and 19.2 mol% ($Co_{0.192}Ni_{0.808}(OH)_2$), as shown in Fig. 2d and e. The loading of composites attached on nickel foam was around 10 ± 0.5 mg cm^{-2}. These results suggested that the $Co_xNi_{1-x}(OH)_2$ composites have been successfully synthesized on nickel foam via this method.

3.2. Supercapacitance performance of the $Co_xNi_{1-x}(OH)_2$ electrode

In order to estimate the electrochemical capacitive properties of $Co_xNi_{1-x}(OH)_2$ composite materials, cyclic voltammetry

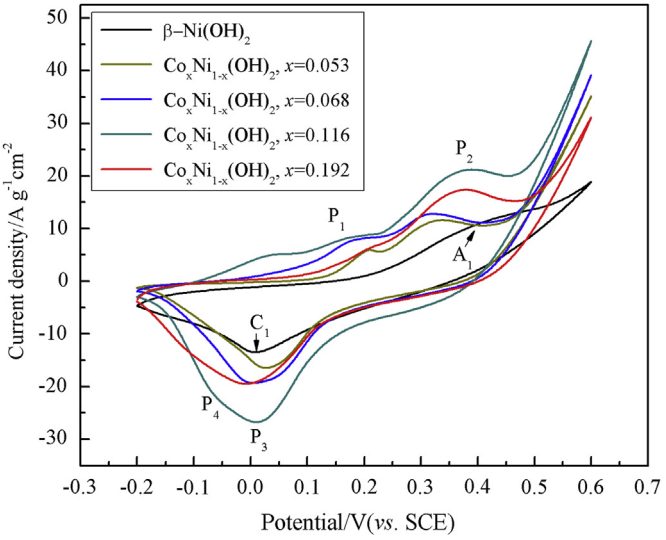

Fig. 3. The CVs of the $Co_xNi_{1-x}(OH)_2$ electrodes at a scan rate of 10 mV s^{-1} in the potential range of −0.2–0.6 V.

experiments in 6 mol dm^{-3} KOH electrolyte at a scan rate of 10 mV s^{-1} were performed, as shown in Fig. 3. For pure β-$Ni(OH)_2$, wide anodic peaks (A_1) and cathodic peaks (C_1) were observed in the potential range of −0.2–0.6 V, corresponding to the transition of the redox couple β-$Ni(OH)_2$/β-NiOOH, as shown in Equation (1). After the addition of Co^{2+}, the obvious anodic peaks (P_1 and P_2) and cathodic peak (P_3 and P_4) were observed. The peaks (P_1 and P_4) occurred at more negative potential position compared to the peaks (A_1 and C_1) can be attributed to the transition of the redox couple Co(III)/Co(II), as shown in Equation (2). While the wide peaks (P_2 and P_3) represents two electrode processes, as shown in Equations (1) and (3). This is due to the similar electrode reactions potential between cobalt and nickel. With the increase of Co^{2+} content in β-$Ni(OH)_2$, the current intensity of anodic peaks and cathodic peaks increases correspondingly. It was found that the current density for $Co_{0.116}Ni_{0.884}(OH)_2$ is highest than that for the pure β-$Ni(OH)_2$ and the other composite materials. Generally, the difference between the oxidation potential and the reduction potential is taken as a measure of the reversibility of the electrode reaction [26]. In the meantime, it is found that the potential difference for the composite materials is smaller than that for pure β-$Ni(OH)_2$ species. Consequently, it can be seen that the reversibility for electrode reaction is greatly improved by the doping of Co^{2+}. Hence, for the $Co_xNi_{1-x}(OH)_2$ electrodes, the electrochemical reversibility and activity for the electrochemical redox reactions should be better. The three pairs of redox reaction are described by the following equations:

$$\beta - Ni(OH)_2 + OH^- \leftrightharpoons \beta - NiOOH + H_2O + e^- \quad (1)$$

$$Co(OH)_2 + OH^- \leftrightharpoons CoOOH + H_2O + e^- \quad (2)$$

$$CoOOH + OH^- \leftrightharpoons CoO_2 + H_2O + e^- \quad (3)$$

Fig. 4 compares the first charge/discharge curves of β-$Ni(OH)_2$ and $Co_xNi_{1-x}(OH)_2$ electrode at a galvanostatic current density of 1 A g^{-1}. It should be pointed out that the oxygen evolution reaction occurred during the charge process, the actual charge/discharge potential range of 0–0.4 V. The curves indicate that most of the capacitance is generated in the potential range of 0–0.4 V, corresponding to the redox reaction of nickel and cobalt hydroxides, as demonstrated in Fig. 3. The addition of Co^{2+} did not affect the charge/discharge curves profiles significantly due to its lower mol content of Co^{2+} in β-$Ni(OH)_2$. For the $Co_xNi_{1-x}(OH)_2$ electrodes, the capacitive characteristic is better than the pure β-$Ni(OH)_2$ electrode. In the sample of $Co_{0.116}Ni_{0.884}(OH)_2$, the highest electrochemical capacitance was observed. These results are in good agreement with the peaks changes as shown in Fig. 3. This could attributed to the unique mixtures structures, which might be favorable to the proton diffusion during the charge/discharge processes.

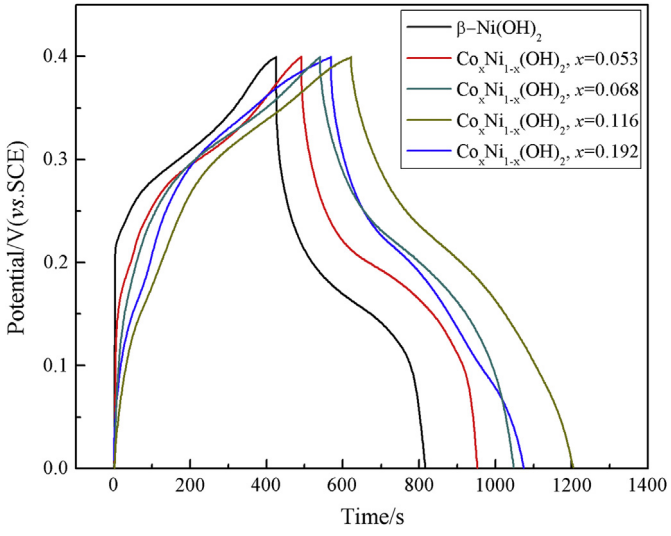

Fig. 4. The charge/discharge curves of the $Co_xNi_{1-x}(OH)_2$ electrodes at a galvanostatic current density of 1 A g^{-1}.

Fig. 5 shows the influence of discharge current density on the specific capacitance of the β-$Ni(OH)_2$, $Co_{0.053}Ni_{0.947}(OH)_2$, $Co_{0.068}Ni_{0.932}(OH)_2$, $Co_{0.116}Ni_{0.884}(OH)_2$ and $Co_{0.192}Ni_{0.808}(OH)_2$ electrode. The specific capacitance was calculated according to the following equation:

$$C_m = \frac{I_d \times \Delta t}{\Delta V} \quad (4)$$

where C_m (F g^{-1}) is the specific capacitance, I_d (A g^{-1}) is the discharge current density, Δt (s) is the discharge time and ΔV (V) is the discharge potential range. The specific capacitances at different discharge current densities were obtained from Fig. 5, and are listed in Table 2. As shown in Table 2, the maximum specific capacitance of pure β-$Ni(OH)_2$ electrode is 1030.2 F g^{-1} at a discharge current density of 1 A g^{-1}. After the addition of Co^{2+}, the specific capacitance of the $Co_xNi_{1-x}(OH)_2$ electrodes is higher than that of pure β-$Ni(OH)_2$ electrode. The $Co_{0.116}Ni_{0.884}(OH)_2$ electrode exhibits highest specific capacitance of 1464.7 F g^{-1} at a current density of 1 A g^{-1}. As shown in Fig. 5f, when the discharge current density increases from 1 A g^{-1} to 6 A g^{-1}, the specific capacitance for pure β-$Ni(OH)_2$ electrode decreases from 1030.2 F g^{-1} to 386.4 F g^{-1}, while that for the $Co_{0.116}Ni_{0.884}(OH)_2$ electrode maintains a high level of 1082.6 F g^{-1}. The capacitance retention was found to be 37.5% and 73.9% for pure β-$Ni(OH)_2$ and $Co_{0.116}Ni_{0.884}(OH)_2$, respectively. In addition, the capacitance was also much better than that of the pure cobalt oxide prepared via this method by our group [23], which exhibited capacitances of 746 F g^{-1} at 5 mA cm^{-2} (0.313 A g^{-1}) and 568 F g^{-1} at 30 mA cm^{-2} (1.875 A g^{-1}). The results showed $Co_{0.116}Ni_{0.884}(OH)_2$ composite electrode exhibited much better electrochemical performances than single Co_3O_4 and $Ni(OH)_2$. Additionally, the capacitances obtained, in our case, are much higher than those of the Co–Ni mixed hydroxide (672 F g^{-1}) prepared by Lokhande's group [27], the cobalt–nickel (Co–Ni) composite thin films (324 F g^{-1}) grown by Kandalkar et al. [28] and the $Co(OH)_2$–$Ni(OH)_2$/USY composite (367 F g^{-1}) prepared by Liang et al. [29]. These results indicate that this $Co_{0.116}Ni_{0.884}(OH)_2$ composite electrode could exhibit higher capacitive properties at high charge/discharge current density.

The $Co_{0.116}Ni_{0.884}(OH)_2$ electrode was subjected to galvanostatic charge/discharge cycling at a current density of 1 A g^{-1} in the potential range of 0–0.4 V, and the cyclic performance was shown in Fig. 6. It can be seen that the discharge capacitance of $Co_{0.116}Ni_{0.884}(OH)_2$ electrode decreases from 1463.6 F g^{-1} to 1257.5 F g^{-1} up to 500 cycles and more than 86% of the initial capacitance can be retained. Furthermore, during the cycling process, the coulombic efficiency remains above 97%.

The capacitive properties of the electrodes were examined further by electrochemical impedance spectroscopy. Fig. 7 shows EIS in the forms of Nyquist plots for β-$Ni(OH)_2$ and $Co_xNi_{1-x}(OH)_2$ composite electrodes. The complex-plane impedance plots for each sample can be divided into the high frequency region and the low frequency region. The diameter of the semicircle at high frequency represents the faradic charge transfer resistance of the redox reactions [30,31]. For the pure β-$Ni(OH)_2$ electrode, charge transfer resistance is estimated around 0.2 Ω cm^{-2}. It can be seen that all the composite electrodes exhibit a small faradic charge transfer

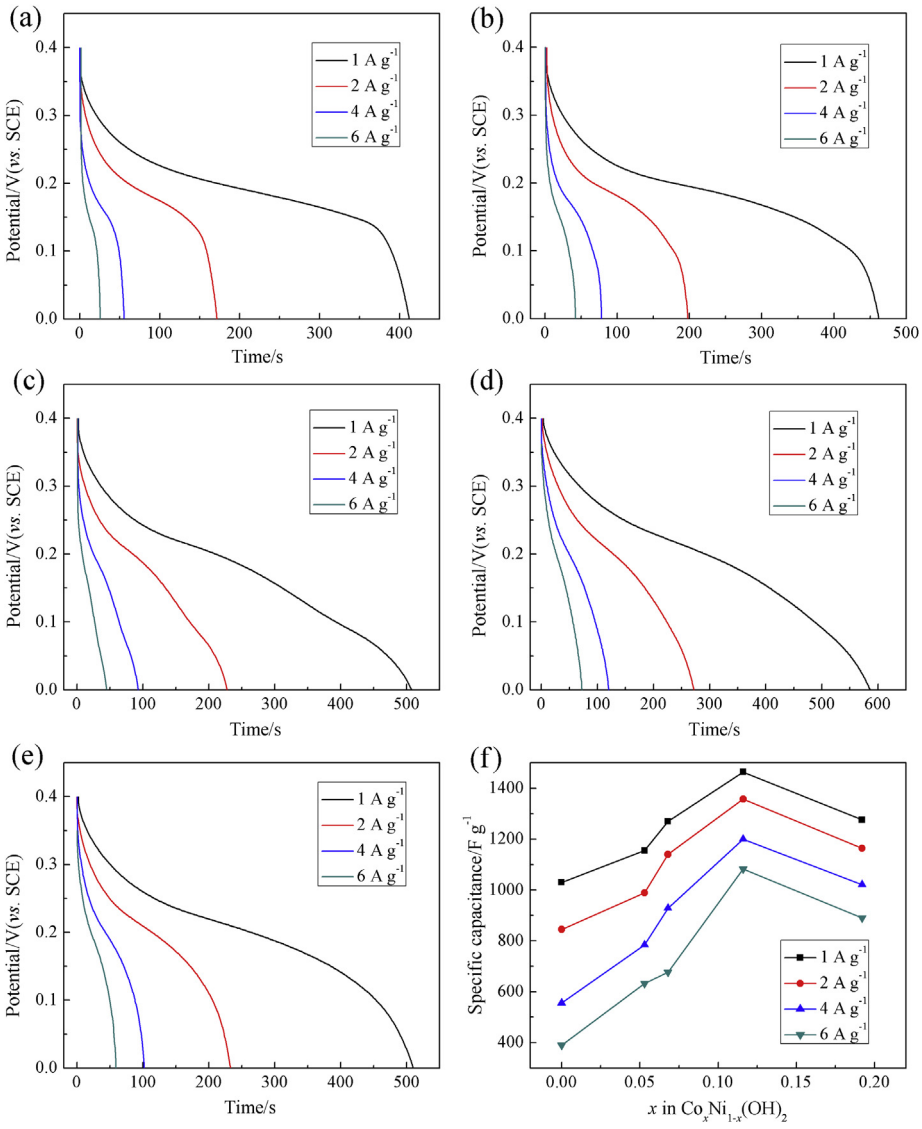

Fig. 5. The discharge curves of the $Co_xNi_{1-x}(OH)_2$ electrodes at different current densities (a) $x = 0$, (b) 0.053, (c) 0.068, (d) 0.116 (e) 0.192; (f) Dependences of the discharge specific capacitance on the charge/discharge current densities and cobalt content.

resistance which was drastically reduced by the additions of Co^{2+}. In the meantime, the charge transfer resistance is about only 0.05 Ω cm^{-2} for both $Co_{0.116}Ni_{0.884}(OH)_2$ and $Co_{0.192}Ni_{0.808}(OH)_2$ electrodes. For all the electrodes, the inclined line in the low frequency region represents the Warburg impedance, which was associated with the ion diffusion of electrolyte. In the sample of $Co_{0.116}Ni_{0.884}(OH)_2$, a straight line of greatest slope at the lower frequency region demonstrates the capacitance nature of the electrode (vertical line for an ideal capacitor). The EIS results show

Table 2
The specific capacitance of the β-$Ni(OH)_2$, $Co_{0.053}Ni_{0.947}(OH)_2$, $Co_{0.068}Ni_{0.932}(OH)_2$, $Co_{0.116}Ni_{0.884}(OH)_2$ and $Co_{0.192}Ni_{0.808}(OH)_2$ electrode at different discharge current densities (corresponding to Fig. 5).

Specific capacitance (F g^{-1})	I_d (A g^{-1})	I_d (A g^{-1})	I_d (A g^{-1})	I_d (A g^{-1})
$Co_xNi_{1-x}(OH)_2$	1	2	4	6
β-$Ni(OH)_2$	1030.2	858.7	556.3	386.4
$x = 0.053$	1154.9	989.2	784.7	631.6
$x = 0.068$	1270.1	1139.7	929.2	676.6
$x = 0.116$	1464.7	1358.4	1200.1	1082.6
$x = 0.192$	1275.5	1164.3	1021.5	890.4

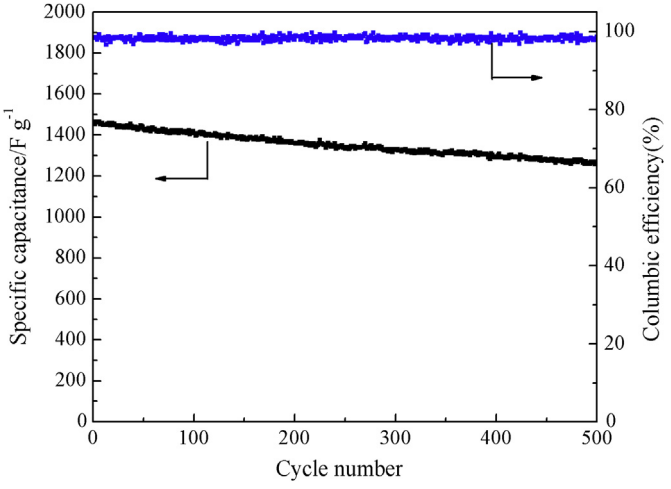

Fig. 6. Dependences of the discharge specific capacitance and the columbic efficiency on the charge/discharge cycle numbers. The charge/discharge tests were performed at 1 A g^{-1} in 6.0 mol dm^{-3} KOH solution.

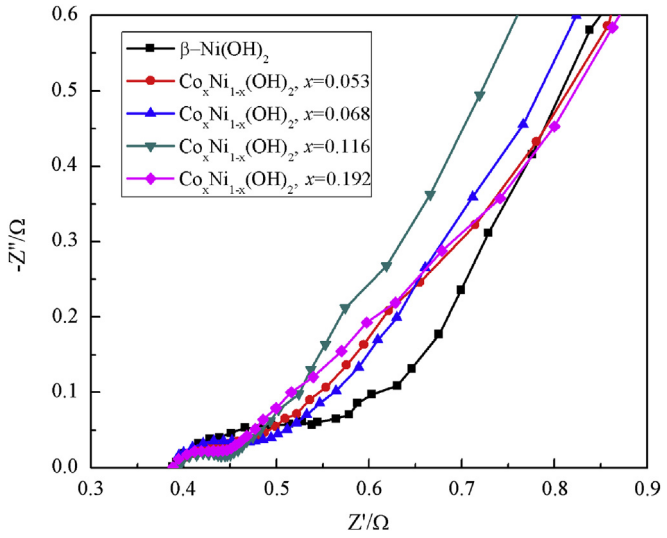

Fig. 7. The electrochemical impedance spectrum of $Co_xNi_{1-x}(OH)_2$ composites electrodes measured at the different potential.

the $Co_{0.116}Ni_{0.884}(OH)_2$ electrode has a lower charge transfer resistance and ion diffusion resistance with fast reaction kinetics.

Recently, it is reported that compounds of mixed oxides/hydroxides composites have superior capacitive performance to single transition metal oxide/hydroxide as electrode [4,27,32]. Generally, they concluded that the superior capacitance is mainly attributed the unique mixture structures. This structure not only provides a fast electron transport path and a large surface area, but also enhances the accessibility of KOH electrolyte and therefore promotes ion transport within the electrode. In this work, we believe that the high electrochemical performances not only come from the unique nanoribbons architecture, but also the synergistic effect between Co and Ni. Firstly, the nanoribbons structure directly attached on nickel foam could shorten the transportation path for both electrons and ions. Secondly, the nanoribbons films possess a favorable morphological stability, which help to alleviate the structure damage caused by volume expansion during the charge/discharge processes. Additionally, the results show that the superior electrochemical reversibility and lower charge transfer resistance for $Co_{0.116}Ni_{0.884}(OH)_2$ composite electrode, leading to fast kinetics. It is also believed that the synergistic effect between Co and Ni lead to the superior capacitive properties at high charge/discharge current density.

4. Conclusion

In summary, nanostructured $Co_xNi_{1-x}(OH)_2$ ($x = 0$, 0.053, 0.068, 0.116, 0.192) composites supported on nickel foam were synthesized via a simple template-free growth method. The specific capacitances of the pure β-$Ni(OH)_2$ electrode were 1030.2, 858.7, 556.3 and 386.4 F g^{-1} at 1, 2, 4 and 6 A g^{-1}, respectively. After the doping of Co^{2+}, it was found that the $Co_{0.116}Ni_{0.884}(OH)_2$ composites electrodes exhibit the highest specific capacitance of 1464.7, 1358.4, 1200.1 and 1082.6 F g^{-1} corresponding to the discharging current densities of 1, 2, 4 and 6 A g^{-1}, respectively. The as-prepared $Co_{0.116}Ni_{0.884}(OH)_2$ electrode has a promising future as higher charging/discharging rate materials for pseudo-supercapacitors.

Acknowledgments

We gratefully acknowledge the financial support of this research by Fundamental Research Funds for the Central Universities (HEUCFT1205), the Postdoctoral Science-Research Developmental Foundation of Heilongjiang Province (LBQ-Q11149), Harbin Science and Technology Innovation Fund for Excellent Academic Leaders (2012RFXXG103) and Specialized Research Fund for the Doctoral Program of Higher Education (20102304110001).

References

[1] J.P. Zheng, T.R. Jow, Journal of Power Sources 62 (1996) 155–159.
[2] M. Winter, R.J. Brodd, Chemical Reviews 104 (2004) 4245–4270.
[3] H. Zhang, G.P. Cao, Z.Y. Wang, Y.S. Yang, Z.J. Shi, Z.N. Gu, Nano Letters 8 (2008) 2664–2668.
[4] V. Gupta, S. Gupta, N. Miura, Journal of Power Sources 175 (2008) 680–685.
[5] G.P. Wang, L. Zhang, J.J. Zhang, Chemical Society Reviews 41 (2012) 797–828.
[6] P. Simon, Y. Gogotsi, Nature Materials 7 (2008) 845–854.
[7] L.L. Zhang, X.S. Zhao, Chemical Society Reviews 38 (2009) 2520–2531.
[8] C.C. Hu, K.H. Chang, M.C. Lin, Y.T. Wu, Nano Letters 6 (2006) 2690–2695.
[9] C.Z. Yuan, X.G. Zhang, L.H. Su, B. Gao, L.F. Shen, Journal of Materials Chemistry 19 (2009) 5772–5777.
[10] J.H. Jiang, A. Kucernak, Electrochimica Acta 47 (2002) 2381–2386.
[11] C. Lin, J.A. Ritter, B.N. Popov, Journal of the Electrochemical Society 145 (1998) 4097–4103.
[12] T. Brezesinski, J. Wang, S.H. Tolbert, B. Dunn, Nature Materials 9 (2010) 146–151.
[13] N.L. Wu, S.Y. Wang, C.Y. Han, D.S. Wu, L.R. Shiue, Journal of Power Sources 113 (2003) 173–178.
[14] L. Nyholm, G. Nystr€om, A. Mihranyan, M. Strømme, Advanced Materials 23 (2011) 3751–3769.
[15] G.W. Yang, C.L. Xu, H.L. Li, Chemical Communications (2008) 6537–6539.
[16] L. Cao, F. Xu, Y.Y. Liang, H.L. Li, Advanced Materials 16 (2004) 1853–1857.
[17] J.C. Huang, J.T. Zhu, K. Cheng, Y. Xu, D.X. Cao, G.L. Wang, Electrochimica Acta 75 (2012) 273–278.
[18] J.C. Huang, H.B. Wu, D.X. Cao, G.L. Wang, Electrochimica Acta 75 (2012) 208–212.
[19] J.P. Liu, J. Jiang, C.W. Cheng, H.X. Li, J.X. Zhang, H. Gong, H.J. Fan, Advanced Materials 22 (2011) 2076–2081.
[20] J.P. Liu, J. Jiang, M. Bosman, H.J. Fan, Journal of Materials Chemistry 22 (2012) 2419–2426.
[21] H. Jiang, C.Z. Li, T. Sun, J. Ma, Chemical Communications 48 (2012) 2606–2608.
[22] J.H. Zhong, A.L. Wang, G.R. Li, J.W. Wang, Y.N. Ou, Y.X. Tong, Journal of Materials Chemistry 22 (2012) 5656–5665.
[23] Y.Y. Gao, S.L. Chen, D.X. Cao, G.L. Wang, J.L. Yin, Journal of Power Sources 195 (2010) 1757–1760.
[24] G.L. Wang, J.C. Huang, S.L. Chen, Y.Y. Gao, D.X. Cao, Journal of Power Sources 196 (2011) 5756–5760.
[25] Y. Wang, D.X. Cao, G.L. Wang, S.S. Wang, J.Y. Wen, J.L. Yin, Electrochimica Acta 56 (2011) 8285–8290.
[26] J. Chen, D.H. Bradhurst, S.X. Dou, H.K. Liu, Journal of the Electrochemical Society 146 (1999) 3606–3612.
[27] D.P. Dubal, A.D. Jagadale, S.V. Patil, C.D. Lokhande, Materials Research Bulletin 47 (2012) 1239–1245.
[28] S.G. Kandalkar, H.M. Lee, S.H. Seo, K. Lee, C.K. Kim, Journal of Materials Science 46 (2011) 2977–2981.
[29] Y.Y. Liang, S.J. Bao, H.L. Li, Journal of Solid State Electrochemistry 11 (2007) 571–576.
[30] D.D. Zhao, W.J. Zhou, H.L. Li, Chemistry of Materials 19 (2007) 3882–3891.
[31] Z.R. Chang, H.W. Tang, J.G. Chen, Electrochemistry Communications 1 (1999) 513–516.
[32] J.M. Luo, B. Gao, X.G. Zhang, Materials Research Bulletin 43 (2008) 1119–1125.